CHEMISTRY
A EUROPEAN JOURNAL

DOI: 10.1002/chem.200700600

Linking Two Distinct Layered Networks of Nanosized $\{Ln_{18}\}$ and $\{Cu_{24}\}$ Wheels through Isonicotinate Ligands

Jian-Wen Cheng,[a] Jie Zhang,[a] Shou-Tian Zheng,[a] and Guo-Yu Yang*[a, b]

Abstract: A new series of heterolanthanide(III)-copper(I) wheel-cluster complexes $[Ln_6(\mu_3\text{-}O)_2](IN)_{18}[Cu_8(\mu_4\text{-}I)_2(\mu_2\text{-}I)_3]\cdot H_3O$ (IN = isonicotinate; Ln = Y **1**, Nd **2**, Dy **3**, Gd **4**, Sm **5**, Eu **6**, Tb **7**) were prepared by hydrothermal reaction at low pH. X-ray crystallographic studies reveal that two unusual trinuclear $[Ln_3(\mu_3\text{-}O)]$ and tetranuclear $[Cu_4(\mu_4\text{-}I)]$ cores are successfully used as secondary building units to make two different nanosized wheels $[Ln_{18}(\mu_3\text{-}O)_6(CO_2)_{48}]^{6-}$, $\{Ln_{18}\}$, and $[Cu_{24}(\mu_4\text{-}I)_6(\mu_2\text{-}I)_{12}]^{6+}$, $\{Cu_{24}\}$, with 12-rings and a diameter of 26.7 and 26.4 Å, respectively. The wheels are further assembled into two-dimensional (2D) $\{Ln_{18}\}$ and $\{Cu_{24}\}$ networks, the linkages between two distinct layered networks of $\{Ln_{18}\}$ and $\{Cu_{24}\}$ wheels by IN pillars along the *c* axis giving a series of unprecedented three-dimensional (3D) sandwich frameworks. To our knowledge, compounds **1**–**7** are the first examples containing two different layered networks of nanosized Ln and transition metal (TM) wheels in wheel-cluster chemistry. The IR, UV/Vis, thermogravimetric analysis (TGA), luminescent, and magnetic properties of these complexes were also studied.

Keywords: cluster compounds · copper · hydrothermal synthesis · lanthanides · open frameworks · porous materials

Introduction

In the past decade, nanoscale wheel clusters have attracted extensive interest due to their fascinating structures and potential applications in nanoscience,[1] host–guest chemistry,[2] supramolecular chemistry,[3] and magnetochemistry[4,5] As a result, many large homometallic cyclic clusters of transition metals (TMs)[3–10] and lanthanides (Ln)[11] have been successfully synthesized. Recently, the synthesis of hetero-TM wheels has undergone great progress, such as isolated $[Fe_6Mn_6]$,[12] $[Cr_mM_n]$ ($m = 6$–10, $n = 1$–2),[13a–g] and dimeric $[Cr_7Ni]_2L$ (L = diamines), and $[Cr_7Ni]_2[M_2]$ (M = Cu, Ni, Co, Ru).[13h,i] However, the analogous chemistry of hetero-Ln-TM wheels is still underdeveloped.

Generally, the choice of ligands is critical to construct and link metal clusters or wheels.[14] Previously we reported the first Ln-TM frameworks, $[Ln_{14}(\mu_6\text{-}O)(\mu_3\text{-}OH)_{20}(IN)_{22}Cu_6X_4(H_2O)_8]\cdot 6H_2O$ (Ln = Y, Gd, Dy, Er, Tb, X = Cl; Ln = Er, Gd, Y, X = Br)[14a] and $[Er_7(\mu_3\text{-}O)(\mu_3\text{-}OH)_6(bdc)_3](ina)_9[Cu_3X_4]$ (**FJ-2, FJ** = Fujian Institute of Research on the Structure of Matter), X = Cl, Br; IN = ina: isonicotinate, bdc = 1,2-benzenedicarboxylate).[14b] The former is based on the linkages of nanosized hydroxo $\{Ln_{14}\}$ clusters and $[Cu_2X_2]$/Cu centers by IN ligands; the latter is based on the links by ina ligands of layered networks, built from $\{Er_{36}\}$ wheels and $[Cu_3X_4]$ cluster cores. Notably, the Ln clusters in the frameworks above change from $\{Ln_{14}\}$ cores to networks made of $\{Er_{36}\}$ wheels owing to the synergistic coordination between both ligands of ina and bdc, whereas the TM clusters form dimeric $[Cu_2X_2]$ to trimeric $[Cu_3X_4]$ cores containing one μ_3-X atom. Based on this chemistry we were intrigued as to whether the size of halogen atoms as inorganic ligands influence the aggregation of metal-halide clusters and whether the larger TM clusters, wheels, or networks of wheels could be introduced in Ln cluster or Ln wheel-cluster polymers under rational conditions.

As a continuation of our search for new open-frameworks built from Ln and TM clusters, we have introduced a larger halogen, iodine, based on the following considerations: the I^- ion has a larger ionic radius than Cl^- and Br^-, and may

[a] J.-W. Cheng, Prof. J. Zhang, S.-T. Zheng, Prof. Dr. G.-Y. Yang
State Key Laboratory of Structural Chemistry
Fujian Institute of Research on the Structure of Matter and
Graduate School of the Chinese Academy of Sciences
Fuzhou, Fujian 350002 (China)
Fax: (+86) 591-8371-0051
E-mail: ygy@fjirsm.ac.cn

[b] Prof. Dr. G.-Y. Yang
State Key Laboratory of Rare Earth Materials and Applications
Peking University, Beijing 100871 (China)

Supporting information for this article is available on the WWW under http://www.chemeurj.org/ or from the author.

favor higher coordination numbers and versatile coordination modes, resulting in a larger TM-halide cluster than $[Cu_2X_2]$[14a] and $[Cu_3X_4]$[14b] cores. Herein, we report seven novel wheel-cluster polymers: $[Ln_6(\mu_3\text{-}O)_2](IN)_{18}[Cu_8(\mu_4\text{-}I)_2(\mu_2\text{-}I)_3]\cdot H_3O$ (**FJ-4**, Ln = Y **1**, Nd **2**, Dy **3**, Gd **4**, Sm **5**, Eu **6**, Tb **7**, respectively). The structures are the first sandwich frameworks based on linkages of two distinct layered networks of nanosized wheels with 12-rings, $[Ln_{18}(\mu_3\text{-}O)_6(CO_2)_{48}]^{6-}$, $\{Ln_{18}\}$, and $[Cu_{24}(\mu_4\text{-}I)_6(\mu_2\text{-}I)_{12}]^{6+}$, $\{Cu_{24}\}$, formed by using IN ligands. To our knowledge, no systematic investigation has been conducted on wheel-cluster polymers in which the distinct networks of metal wheels, especially where two networks of Ln and TM wheels are linked to together by organic ligands, except for two Ln and two TM wheel-cluster polymers containing layered networks of $\{Er_{36}\}$,[14b] $\{Mo_{154}\}$,[15a] and $\{Mo_{152}\}$[15b] wheels.

Results and Discussion

Red prismatic crystals of **1–7** were obtained in the hydrothermal reaction of Ln_2O_3, CuI, HIN, and 2-pyrazinecarboxylic acid (pca) in water in the presence of $HClO_4$ (pH 2). In addition, light yellow rectangular crystals were also obtained at the same time.[16] X-ray structure analyses reveal that **1–7** are isomorphous and crystallize in the high-symmetry rhombohedral space group $R\bar{3}c$ (Table 1). Therefore, only the structure of **3** is described in detail. The asymmetric unit of **3** contains one unique Dy^{3+}, two Cu^+, two I^- ions, and three IN ligands with only one coordination mode (Figure 1a, Scheme 1). The Dy^{3+} ion is seven-coordinate and has a capped trigonal prism coordination geometry: one μ_3-O, and six carboxylate oxygen atoms (O_{COO^-}) from six bridging IN ligands (Figure 1b). The Dy–O bond lengths range from 2.261(5) to 2.372(5) Å. The general trend of decreasing Ln–O distances with increasing atomic number has been observed throughout the series of compounds in line with the lanthanide contraction effect (Table 2).

Three Dy^{3+} ions are linked by one μ_3-O group to give a trinuclear core of $[Dy_3(\mu_3\text{-}O)]$ that was further stabilized by six carboxyl groups of six IN ligands, forming a $[Dy_3(\mu_3\text{-}O)(CO_2)_6]$, $\{Dy_3\}$, cluster (Figure 2a,b). This type of corner-sharing trimeric oxo-centered carboxylate-bridged cluster formulated as $[M_3(\mu_3\text{-}O)(O_2CR)_6]^+$ is well known for Al^{3+}

Table 1. Crystal data and structure refinements for complexes **1–7**.

	1	**2**	**3**	**4**
formula	$C_{108}H_{75}Cu_8Y_6I_5N_{18}O_{39}$	$C_{108}H_{75}Cu_8Nd_6I_5N_{18}O_{39}$	$C_{108}H_{75}Cu_8Dy_6I_5N_{18}O_{39}$	$C_{108}H_{75}Cu_8Gd_6I_5N_{18}O_{39}$
M_r	3925.14	4257.12	4366.68	4335.18
crystal system	rhombohedral	rhombohedral	rhombohedral	rhombohedral
space group	$R\bar{3}c$	$R\bar{3}c$	$R\bar{3}c$	$R\bar{3}c$
a[Å]	15.222(3)	15.3844(6)	15.2435(3)	15.2988(4)
c[Å]	93.80(3)	93.975(8)	93.897(3)	93.559 (4)
V[Å^3]	18820(7)	19262(2)	18895.2(8)	18964.1(10)
Z	6	6	6	6
ρ[g cm^{-3}]	2.078	2.202	2.303	2.278
μ[mm^{-1}]	5.381	4.959	6.141	5.720
F(000)	11352	12108	12324	12252
GOF	1.15	1.237	1.238	1.174
collected reflns	44806	47404	16252	15593
unique reflns (R_{int})	4816(0.0556)	4920(0.0493)	4791(0.0305)	4803(0.0302)
observed reflns [$I > 2\sigma(I)$]	4428	4688	4173	4134
refined parameters	278	278	279	278
R_1[a]/wR_2[b] [$I > 2\sigma(I)$]	0.0444/0.1433	0.0462/0.1129	0.0436/0.1203	0.0349/0.0978
R_1[a]/wR_2[b] (all data)	0.0567/0.1584	0.0489/0.1145	0.0556/0.1412	0.0449/0.1174

	5	**6**	**7**
formula	$C_{108}H_{75}Cu_8Sm_6I_5N_{18}O_{39}$	$C_{108}H_{75}Cu_8Eu_6I_5N_{18}O_{39}$	$C_{108}H_{75}Cu_8Tb_6I_5N_{18}O_{39}$
M_r	4293.78	4303.44	4345.20
crystal system	rhombohedral	rhombohedral	rhombohedral
space group	$R\bar{3}c$	$R\bar{3}c$	$R\bar{3}c$
a[Å]	15.3539(4)	15.3029(4)	15.274(2)
c[Å]	93.851(5)	93.566(5)	93.866(18)
V[Å^3]	19160.5(13)	18975.7(12)	18966(5)
Z	6	6	6
ρ[g cm^{-3}]	2.233	2.260	2.283
μ[mm^{-1}]	5.305	5.546	5.929
F(000)	12180	12216	12288
GOF	1.214	1.188	1.182
collected reflns	45604	12571	46783
unique reflns (R_{int})	4892 (0.0428)	4843 (0.0306)	4850 (0.0473)
observed reflns [$I > 2\sigma(I)$]	4658	3885	4462
refined parameters	278	279	278
R_1[a]/wR_2[b] [$I > 2\sigma(I)$]	0.0420/0.1127	0.0420/0.1141	0.0316/0.0875
R_1[a]/wR_2[b] (all data)	0.0446/0.1143	0.0574/0.1388	0.0356/0.0898

[a] $R_1 = \Sigma||F_o| - |F_c||/\Sigma|F_o|$. [b] $wR_2 = \{\Sigma[w(F_o^2 - F_c^2)^2]/\Sigma[w(F_o^2)^2]\}^{1/2}$.

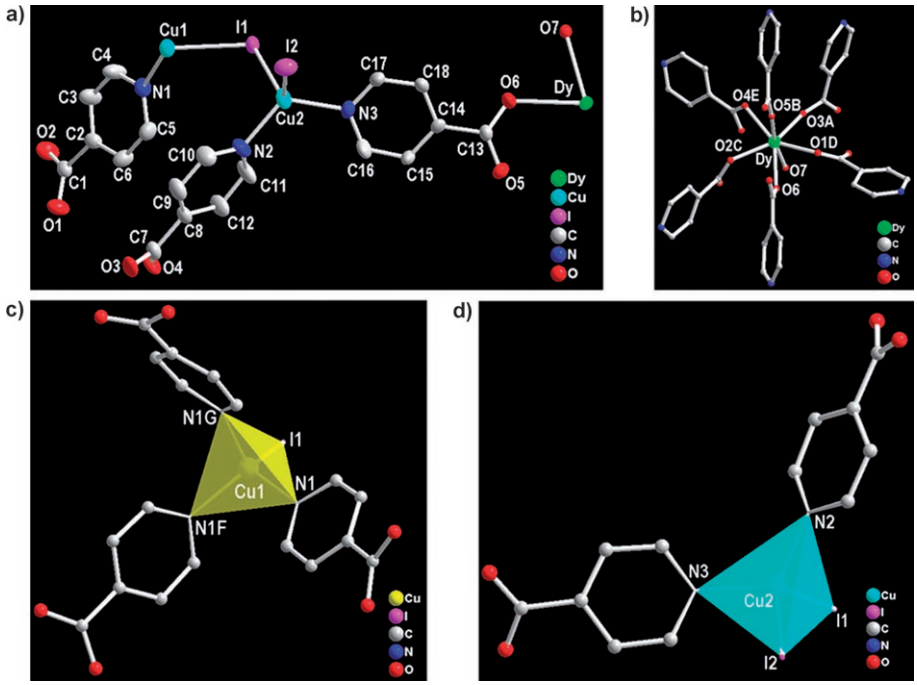

Figure 1. a) The asymmetrical unit of compound **3**; b) the coordination environments of Dy atom in **3**; c) the coordination environments of the Cu1 atom: one I and three N atoms from three IN ligands with mode I. Cu1–I1: 2.631(2), Cu1–N1: 2.122(6) Å; d) the coordination environments of the Cu2 atom: two I and two N atoms from two IN ligands with mode II and III, respectively. Cu2–I1: 2.801(1), Cu2–I2: 2.630(1), Cu2–N: 2.016(5)–2.039(5) Å. Atoms with A, B, C, D, E, F, and G in their labels are symmetry-generated. Symmetry code A: $-x+y+1/3$, $y-1/3$, $z+1/6$; B: $-x+5/3$, $-y+7/3$, $-z+4/3$; C: $y+1/3$, $x+2/3$, $-z+7/6$; D: $-x+4/3$, $-x+y+2/3$, $-z+7/6$; E: $x+1/3$, $x-y+5/3$, $z+1/6$; F: $-y+2$, $x-y+1$, z; G: $-x+y+1$, $-x+2$, z.

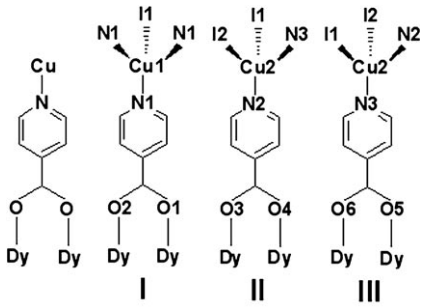

Scheme 1. Coordination modes of the IN and its three linking modes (I–III) in **3**. Modes I–III containing N1/O1/O2, N2/O3/O4, and N3/O5/O6 atoms, respectively.

and many trivalent TMs,[17] but it is observed for the first time in Ln chemistry. So far, only several trimeric Ln complexes with a different configuration were reported, in which each Ln ion shares a triangular face with the other two.[18] Six $\{Dy_3\}$ clusters are further linked by twelve carboxyl groups of twelve IN ligands to form a nanosized $\{Dy_{18}\}$ wheel with a 12-ring and the diameter of 26.7 Å (Figure 2c–e), which is another novel nanosized Ln wheel that remarkably differs from the $\{Er_{36}\}$[14b] wheel in linkage modes. Compared with TM wheels containing trinuclear building blocks, the $\{Ni_{24}\}$[5a]/$\{Fe_{18}\}$[7b] wheels can be described as an oligomer of eight/six trinuclear building blocks, whereas each $\{Dy_{18}\}$ wheel is linked to the adjacent wheels by sharing $\{Dy_3\}$ bridging building blocks, resulting in a highly ordered layered $\{Dy_{18}\}$ wheel-cluster network with hexagonal, honeycomb arrays (Figure 2 f). Notably, the previously reported Ln wheels are formed not only by bridging organic ligands, but also by sharing Ln ions. In $\{Ln_8\}$/$\{Ln_{10}\}$/$\{Ln_{12}\}$ wheels, for example, the Ln ions are linked by ligands with the O atom donor to form 8-/10-/12-rings in which the center is empty;[11a,f,g,h] whereas in $\{Ln_{12}\}$/$\{Ln_{15}\}$ wheels, four or five $\{Ln_4\}$ cores share Ln vertices to form 4-/5-rings with one or two halide ions in their central cavity.[11c,d] Remarkably, the construction mode of the wheel-shaped $\{Dy_{18}\}$ reported here is significantly different from the above-mentioned discrete Ln wheels. The $\{Dy_{18}\}$ wheel with a 12-ring is made up of six

Table 2. Selected bond lengths [Å] for **1**–**7**.[a]

	1	**2**	**3**	**4**	**5**	**6**	**7**
Ln–O3#1	2.244(4)	2.386(5)	2.261(5)	2.300(5)	2.348(4)	2.319(5)	2.283(4)
Ln–O5#2	2.258(4)	2.381(5)	2.276(5)	2.312(4)	2.341(4)	2.323(5)	2.295(4)
Ln–O2#3	2.312(4)	2.401(5)	2.332(5)	2.355(4)	2.374(4)	2.360(5)	2.344(4)
Ln–O6	2.335(4)	2.453(5)	2.371(5)	2.401(5)	2.421(4)	2.415(5)	2.379(4)
Ln–O1#4	2.342(4)	2.437(5)	2.363(5)	2.386(4)	2.414(4)	2.389(5)	2.375(4)
Ln–O4#5	2.355(4)	2.460(5)	2.372(5)	2.404(5)	2.436(5)	2.409(5)	2.390(4)
Ln–O7	2.364(1)	2.436(2)	2.368(2)	2.391(2)	2.414(2)	2.397(2)	2.381(1)
Cu1–N1	2.129(4)	2.115(6)	2.122(6)	2.115(5)	2.109(5)	2.107(6)	2.118(4)
Cu1–I1	2.631(1)	2.615(2)	2.631(2)	2.619(2)	2.622(1)	2.618(2)	2.626(1)
Cu2–N2	2.008(4)	2.008(5)	2.016(5)	2.017(5)	2.020(5)	2.023(5)	2.018(4)
Cu2–N3	2.035(4)	2.047(5)	2.039(5)	2.043(5)	2.042(5)	2.036(5)	2.046(4)
Cu2–I2	2.6310(9)	2.628(1)	2.630(1)	2.624(1)	2.628(1)	2.625(1)	2.630(1)
Cu2–I1	2.798(1)	2.829(1)	2.801(1)	2.808(1)	2.816(1)	2.810(1)	2.804(1)

[a] Symmetry codes: #1: $-x+y+1/3$, $y-1/3$, $z+1/6$, #2: $-x+5/3$, $-y+7/3$, $-z+4/3$, #3: $y+1/3$, $x+2/3$, $-z+7/6$, #4: $-x+4/3$, $-x+y+2/3$, $-z+7/6$, #5: $x+1/3$, $x-y+5/3$, $z+1/6$.

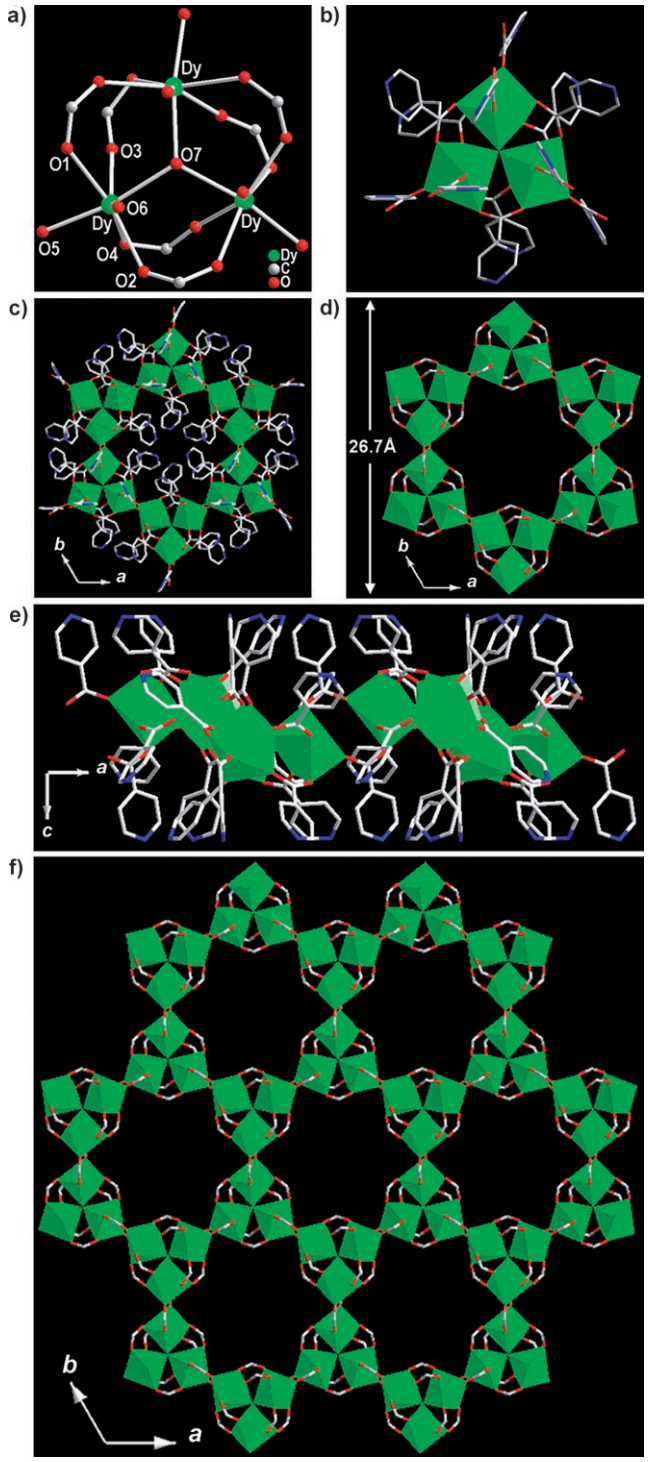

Figure 2. a) The trimeric $\{Dy_3(\mu_3\text{-}O)(CO_2)_6\}$ cluster unit. The pyridine rings of IN ligands are omitted for clarity. b) The polyhedral view of coordination environments of the trimeric $[Dy_3(\mu_3\text{-}O)]$ core in **3**. Twelve IN ligands: Three, three, and six IN ligands with modes I, II, and III, respectively. c) Top view of the coordination environments of $\{Dy_{18}\}$ wheel cluster. A 60-IN-ligand-linked single $\{Dy_{18}\}$ wheel: 18, 18, and 24 IN ligands with modes I, II, and III, respectively. d) Polyhedral view of nanosized $\{Dy_{18}\}$ wheels. The IN ligands were omitted for clarity. e) Side view of the coordination environments of the $\{Dy_{18}\}$ wheel with 60 IN ligands. f) Polyhedral view of layered network of $\{Dy_{18}\}$ wheels.

$\{Dy_3\}$ cores linked by the bridging IN ligands, each $\{Dy_{18}\}$ is linked to surrounding wheels by sharing $[Dy_3(\mu_3\text{-}O)]$, forming a highly ordered layered wheel-cluster network. Additionally, the layered $\{Dy_{18}\}$ wheel is also remarkably different from the layered $\{Er_{36}\}$ wheel in **FJ-2**.[14b] The $\{Er_{36}\}$ wheel in **FJ-2** is made up of strictly alternating $\{Er_4\}$ and $\{Er_2\}$ cores sharing μ_3-OH groups, whereas the bdc ligands are trapped in the 18-ring to further stabilize the $\{Er_{36}\}$ wheel. Each $\{Er_{36}\}$ wheel is linked to surrounding wheels by sharing -Er1-OH-$\{Er2\}_2$-OH-Er1- bridges, forming a highly ordered layered wheel-cluster network.[14b]

Two Cu centers in **3** are four-coordinate in distorted tetrahedral geometries with different coordination environments, comprising one μ_4-I1 and three N atoms from three bridging IN moieties for $Cu1N_3I$, and one μ_4-I1, one μ_2-I2, and two N atoms from two bridging IN ligands for $Cu2N_2I_2$ tetrahedra (Figure 1c,d, Figure 3a); the Cu–I and Cu–N bond lengths range from 2.630(1)–2.801(1) Å and 2.016(5)–2.122(6) Å, for the two tetrahedra, respectively.

Four Cu ions are bridged by corner-sharing one μ_4-I1 atom to form an unprecedented tetrameric I-centered tetrahedral $[Cu_4(\mu_4\text{-}I)]$, $\{Cu_4\}$, cluster core (Figure 3a,b) that differs from the reported tetragonal pyramid of $\{Cu_4\}$, in which the μ_4-I atom is the vertex.[19] Six $\{Cu_4\}$ cores are linked by six μ_2-I2 atoms to form another nanosized $\{Cu_{24}\}$ wheel with a 12-ring and a diameter of 26.4 Å (Figure 3c–e). Compared with the $\{Cu_4\}$ core here, the $\{Cu_3\}$ cores in **FJ-2** are not linked to each other.[14b] In addition, the cyclic $\{Cu_{24}\}$ cluster is the largest halide-bridged Cu wheel to date.[6a] Notably, six Cu1-centered tetrahedra are grouped into threes to form triangles with reverse orientation that are linked on two sides of the 12-ring in the *ab* plane. Adjacent $\{Cu_{24}\}$ wheels are further linked to each other by μ_2-I2 atoms, forming another layered network of $\{Cu_{24}\}$ wheels, with hexagonal honeycomb arrays (Figure 3f, Figure 4). Generally, it is not possible to form a large 3d metal wheel with only one type of bridging interaction.[5a,7c] For example, the famous "ferric wheel" can be accurately described as $[\{Fe(OMe)_2(O_2CR)\}_{10}]$ (R = Me, CH_2Cl, $CH_2CH_2C(O)C_6H_4Me$),[7a,c] a series of Cu^{II} wheels can be summarized as $[\{Cu(OH)(pz)\}_n]$ (pz = pyrazololato anion, $C_3H_3N_2^-$; n = 6, 8, 9, 12, 14),[6b] and a family of heterometallic octanuclear wheels can be formulated as $[M_7M'F_8(O_2CR)_{16}]$ (M = a trivalent metal of Cr, Fe, V, Al, Ga, or In; M′ = a divalent metal of Mn, Fe, Co, Ni, Mg, Zn, Cd; O_2CR = one of around twenty carboxylates),[13j] an so on, these discrete TM wheels are linked by two different bridges. Therefore, the construction mode of the layered wheel-shaped $\{Cu_{24}\}$ in **FJ-4** is significantly different from the above-mentioned discrete TM wheels. In **FJ-4**, the $\{Cu_{24}\}$ wheel only bridged by I atoms is unprecedented. In contrast to other TM wheels based on edge-sharing metal tetrahedra,[7d,e] the $\{Cu_{24}\}$ wheel comprises two different tetrahedra of $Cu1N_3I$ and $Cu2N_2I_2$ through shared vertices. Such a $\{Cu_{24}\}$ wheel with a 12-ring and corner-sharing tetrahedra is analogous to zeolite/zeolite-like open-frameworks,[20] in which the O atoms are usually bi- or tricoordinate. Unlike the I-centered tetrahedra in $\{Cu_{24}\}$ wheel net-

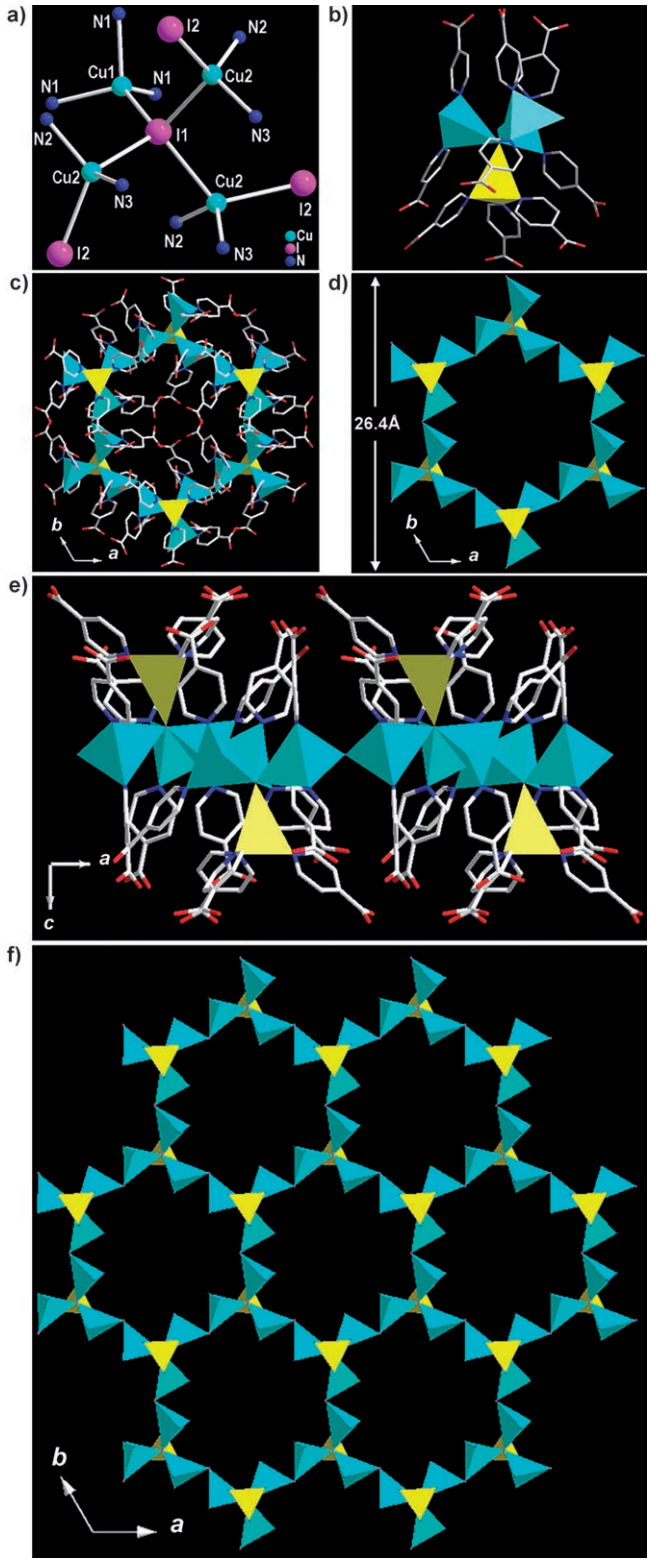

Figure 3. a) The tetrameric [$Cu_4(\mu_4$-I)] cluster core linked by corner-sharing a centered μ_4-I atom. b) Side view of the coordination environment of [$Cu_4(\mu_4$-I)] core in **3**. Nine IN ligands: three, three, and three with modes I, II, and III, respectively. c) Top view of the coordination environment of {Cu_{24}} wheel in **3** along the *c* axis. 54 IN ligands linkedto the single {Cu_{24}} wheel: 18, 18, and 18 IN ligands with modes I, II, and III, respectively. d) Polyhedral view of layered network of {Cu_{24}} wheels. Except for N atoms, other atoms of IN ligands are omitted for clarity. e) Side view of the coordination environment of {Cu_{24}} wheel with 54 IN ligands in **3**. f) Polyhedral view of layered network of {Cu_{24}} wheels. Polyhedral centered by Cu1 (yellow) and Cu2 (cyan).

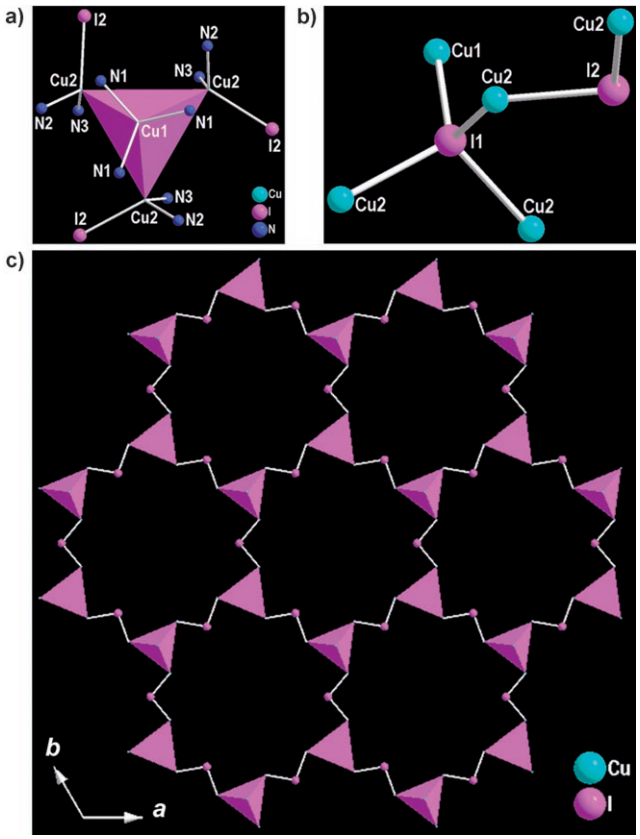

Figure 4. a) The I-centered tetrahedron of [ICu_4] in **3**. Purple denotes the $I1Cu_4$ tetrahedron. b) The coordination environment of I1 and I2 atoms in **3**. I1 and I2 atoms are four and two coordination numbers, respectively. c) View of 2D layered honeycomb network of {Cu_{24}} wheels made of [ICu_4] tetrahedra (purple) and I2 bridges with 12-rings along the *c* axis in **3**.

works, tetrahedrally coordinated O atoms are unusually encountered in zeolite and oxide frameworks due to the small size of the O atom.[21] Compared with our previously reported Ln–organic–TM frameworks containing small TM–halide clusters of [Cu_2X_2][14a] and [Cu_3X_4][14b] cores ($X = Cl^-$ and Br^-), the larger size of the I^- ions is critical for the formation of the {Cu_{24}} wheel networks of **FJ-4**. In addition, the {Mo_{154}}[15a] and {Mo_{152}}[15b] wheels are formed based on the linkages between polyhedra through sharing vertices and edges, but all the polyhedra are octahedra and pentagonal bipyramids, with no tetrahedra in such huge wheels. Also no μ_4-O atoms and [OMo_4] tetrahedra, unlike μ_4-I atoms and [ICu_4] tetrahedra in **FJ-4**, exist in the {Mo_{154}}/{Mo_{152}}[15] wheels because of steric effects, that is, the small/large size for O/Mo atoms, respectively. Like the {Er_{36}} wheel-cluster networks formed in **FJ-2** due to the synergistic coordination between two different organic ligands,[14b] the {Cu_{24}} wheel-cluster networks in **FJ-4** can also be described as the generation under the synergistic coordination between

two kinds of ligands, inorganic iodine and organic isonicotinate.

The linkages between two distinct layered networks of {Ln_{18}} and {Cu_{24}} wheels by IN pillars along the *c* axis, leads to an unprecedented 3D sandwich framework (Figure 5a,b) with multidimensional channels along the [48$\bar{1}$], [44$\bar{1}$], [841], and [88$\bar{1}$] directions (Figure 5c). The channels are filled with protonated water molecules for the charge balance. In addition, the layered networks of {Dy_{18}} and {Cu_{24}} wheels are stacked along the [22$\bar{1}$] direction to form two types of hexagonal channels that interpenetrate (Figure 6). With one of the largest unit-cell dimensions ($c = 93.975$ Å) among all non-protein structures, both layered networks of {Dy_{18}} and {Cu_{24}} wheels are stacked in parallel with -ABCDEF- alternations along the *c* axis, each layer is shifted by ($-\boldsymbol{a}/3+\boldsymbol{b}/3+\boldsymbol{c}/6$) with respect to the next one (Figure 5a,b). Remarkably, the structure of **3** consists of strictly alternating {Dy_{18}} and {Cu_{24}} wheel-cluster networks pillared by IN ligands to form a 3D framework, in which adjacent layered networks of {Cu_{24}}/{Dy_{18}} wheels have opposite orientations along the *c* axis. The distance between two adjacent layers of {Dy_{18}}/{Cu_{24}} wheels, and between adjacent layers of {Dy_{18}} and {Cu_{24}} wheels is 15.65 and 7.82 Å, respectively (Figure 5b). As many as 60 IN ligands are bonded to the {Dy_{18}} wheel: six {Cu_{24}} wheels cap two sides of the {Dy_{18}} wheel through 18 IN (mode I), and other 42 IN ligands (modes II and III) are bonded to Cu1 and Cu2 atoms. Whereas six {Dy_{18}} wheels cap two sides of the {Cu_{24}} wheel through 54 IN ligands: 36 ina ligands (modes I and II) are only coordinated to interior [$Dy_3(\mu_3\text{-O})$] cores, which are further bridged and linked through another 18 IN ligands (mode III).

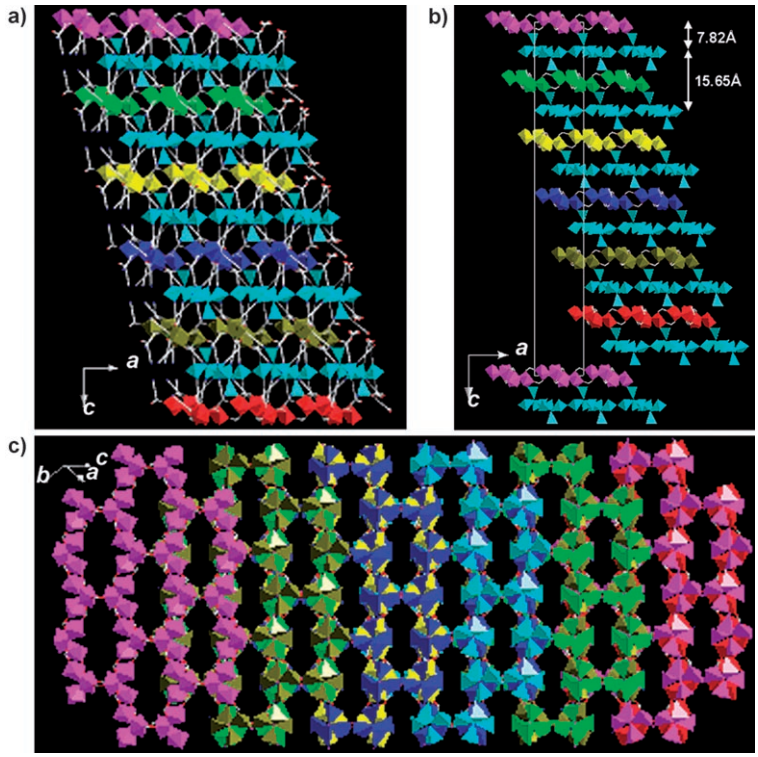

Figure 5. a) View of the layered networks of {Dy_{18}} and {Cu_{24}} wheels stacked in parallel with -ABCDEF- alternations along the *c* axis, each layer is shifted by ($-\boldsymbol{a}/3+\boldsymbol{b}/3+\boldsymbol{c}/6$) with respect to the next one, respectively. Six layers of {Ln_{18}} wheels, A–F, are represented in purple, green, yellow, blue, deep yellow, and red, respectively, whereas each of five layered networks of {Cu_{24}} wheels are located between two adjacent {Dy_{18}} wheel cluster layers shown in cyan for clarity. The pyridine rings of IN ligands are shown with white lines. b) The sandwich framework based on linkages of layered networks of {Dy_{18}} and {Cu_{24}} wheels pillared by IN ligands along the *c* axis. The pyridine rings are omitted for clarity. c) The multidimensional channels stacked by layered networks of {Dy_{18}}/{Cu_{24}} wheels in **3** along different directions, showing an alternate arrangement of the layered networks of the {Dy_{18}} and {Cu_{24}} wheels. Only the channels along the [44$\bar{1}$] direction are shown. From left to right, six networks of {Dy_{18}} wheels are represented in purple, green, green, yellow, blue, deep yellow, and red, while five networks of {Cu_{24}} wheels located between adjacent networks of {Dy_{18}} wheels are represented in deep yellow, blue, cyan, green, and purple, respectively.

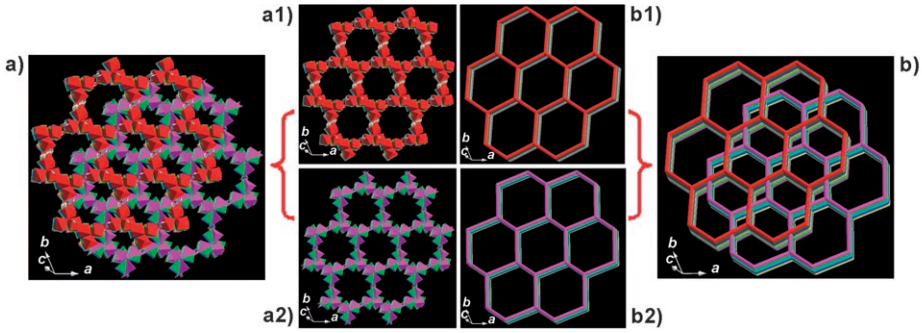

Figure 6. a) Polyhedral view of two types of hexagonal channels, stacked by the layered networks of {Dy_{18}} and {Cu_{24}} wheels along the [22$\bar{1}$] direction, that interpenetrate each other; a1/a2) Polyhedral view of the hexagonal channels stacked by layered networks of {Dy_{18}} and {Cu_{24}} wheels in **3** along the [22$\bar{1}$] direction, respectively; b) topological view of two types of interpenetrating channels covered by red and purple nets are stacked by the layered networks of {Dy_{18}} and {Cu_{24}} wheels along the [22$\bar{1}$] direction, respectively. The {Dy_3} and {Cu_4} cores act as three-connected nodes, respectively; b1/b2) topological view of the hexagonal channels stacked by layered networks of {Dy_{18}} and {Cu_{24}} wheels in **3** along the [2 −2 1] direction, respectively.

Thermal properties: The thermal stabilities of **1**–**7** were examined by the TG analysis in dry-air atmosphere. On account of the isomorphic features of **1**–**7**, **1** as a typical example is described in detail. The TG curve of **1** shows a weight loss of 0.65% (calcd 0.48%) from 30 to 300°C, which corresponds to the release of a protonated water molecule. Between 300 and 600°C, the weight loss corresponds to the decomposition of IN ligands and assuming that the residue corresponds to $3Y_2O_3{\cdot}8CuO$, the observed weight (33.92%) is in good agreement with the calculated value (33.47%). The TG curves of **2**–**7** are similar to that of **1**, the weight loss of protonated water is 0.86, 1.23, 0.73, 1.1, 0.84, and 1.2%, for **2**–**7** (calcd 0.45, 0.43, 0.44, 0.44, 0.44, and 0.44%), respectively. Assuming that the residue corresponds to $3Ln_2O_3{\cdot}8CuO$ (Ln = Nd, Dy, Gd, Sm, Eu) and $3/2Tb_4O_7{\cdot}8CuO$ for **2**–**7**, the residual weights of 39.61, 40.50, 38.61, 39.65, 38.66, and 39.69% in **2**–**7** are in good agreement with the calculated values 38.66, 40.20, 39.76, 39.18, 39.32, and 40.46%, respectively (see Figure S1 in the Supporting Information).

IR spectroscopy: The IR spectra of **1**–**7** are similar. The characteristic features of the IN ligand dominate the IR spectrum. The strong and broad absorption bands in the range of 3000–3700 cm^{-1} in **1**–**7** are assigned as characteristic peaks of OH vibrations. The strong vibrations appearing at 1582 and 1402 cm^{-1} correspond to the asymmetric and symmetric stretching vibrations of the carboxylate group, respectively. The absence of strong bands in the range 1690–1730 cm^{-1} indicate IN ligands are deproponated (see Figure S2 in the Supporting Information).

Optical properties: The optical absorption spectrum reveals that **1**–**7** exhibit strong and similar optical absorption in the visible region, with optical band gaps of 2.19, 2.17, 2.17, 2.12, 2.07, 2.21, and 2.23 eV, respectively, these band gap sizes are significantly smaller than CuI (2.92 eV) (see Figure S3 in the Supporting Information). Thus, a much larger fraction of visible light is absorbed by these lanthanide-containing heterometallic complexes.

Luminescence properties: The profiles of the emission bands for **2** are in agreement with previously reported spectra of Nd^{3+} complexes.[22] Under excitation of 476 nm, **2** displays the characteristic emission bands for the Nd^{3+} ion in the near-IR region: the strongest emission band is at 1058 nm ($^4F_{3/2}\rightarrow{}^4I_{11/2}$) and a weak band is found at 1330 nm ($^4F_{3/2}\rightarrow{}^4I_{13/2}$). Compounds **3**, **5**, **7** show similar broad fluorescent emission spectra from 450 to 800 nm in the solid state, with an intense emission occurring around 650 nm when excited at 420, 438, and 320 nm, respectively, at room temperature (Figure 7). According to the results of the similar copper(I) halide clusters, the emission band might be assigned to a combination of iodide-to-copper charge transfer (LMCT) and d–s transitions by Cu–Cu interaction within Cu_{24} clusters.[23] The fluorescence spectrum of complex **6** was also measured in the solid state at room temperature, the excitation wavenumber was selected as the maximum of the solid-state excitation spectrum at 280 and 357 nm, but no useful emission spectra were observed.

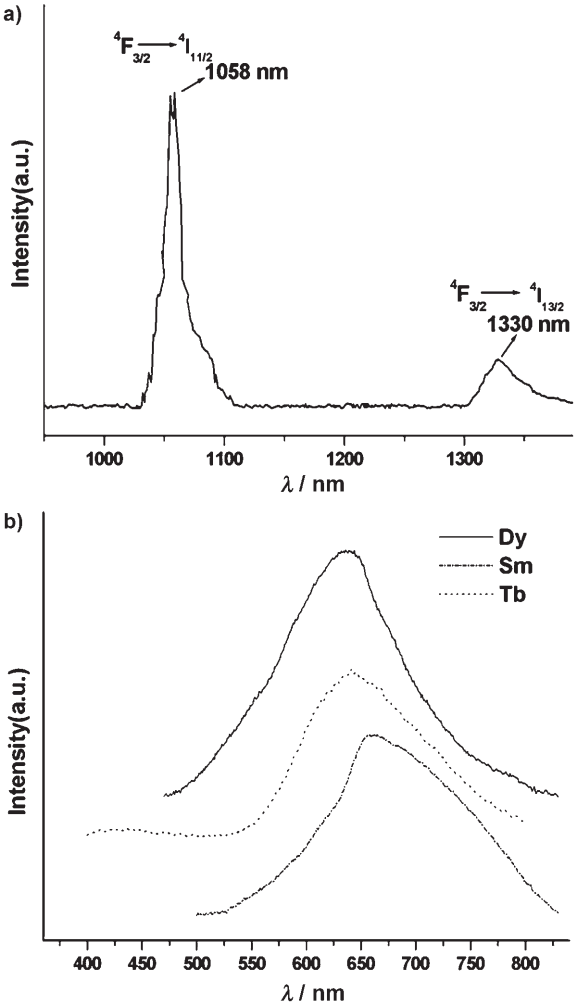

Figure 7. Emission spectra of: a) Compound **2**; b) Compounds **3**, **5**, and **7** in the solid state at room temperature when excited at 476, 420, 438, and 320 nm, respectively.

Magnetic properties: The magnetic susceptibilities of powdered samples of **1**–**4** were measured in the temperature range 2–300 K. The molar magnetic susceptibility of **1** is negative and independent of temperature within 50–300 K, consistent with the assigned structure containing diamagnetic Cu^+ and Y^{3+} ions. At room temperature, the $\chi_M T$ value is equal to 9.87, 84.9, and 46.62 cm^3mol^{-1} K for **2**–**4** (Figure 8), respectively, which are close to the expected values of 9.84, 85.02, and 47.28 cm^3mol^{-1} K for six noninteracting Ln^{3+} ions. On lowering the temperature, the $\chi_M T$ value of **2** decreases monotonically and finally reaches 3.64 cm^3mol^{-1} K at 2 K. Such a magnetic behavior is typical for Nd^{3+} complexes due to the populations of the Stark levels and a weak antiferromagnetic interaction between Nd^{3+} ions.[24] For **3**, $\chi_M T$ decreases slowly with decreasing the temperature to about 50 K and then more rapidly below 50 K, reaching a

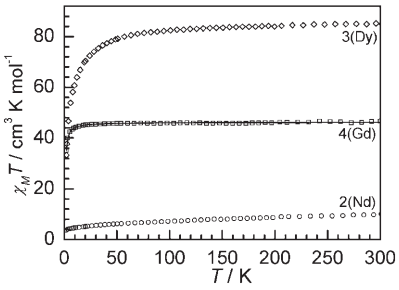

Figure 8. Temperature dependence of the $\chi_M T$ product for **2**, **3**, and **4**. The solid line is the best fit of the data based on the model described in the text for **4**.

value of 33.35 $cm^3 mol^{-1}$ K at 2 K. This behavior might be considered as a result of the ligand field splitting of the Dy^{3+} ions together with a contribution from the weak antiferromagnetic coupling within the {Dy_{18}} cluster unit. The thermal variation of $\chi_M T$ of **4** is similar to that of **3**, and almost obeys the Curie–Weiss law over the whole temperature range with a negative Weiss constant (θ) of −0.61 K and the Curie constant of 46.3 $cm^3 mol^{-1}$ K. Considering the shorter Gd···Gd separations within the μ_3-O bridged trinuclear core of {Gd_{18}} cluster, and a stronger ability of μ_3-O bridge to mediate magnetic coupling than that of *syn–anti* carboxylate bridge linking trinuclear cores, the magnetic susceptibility data of **4** were analyzed approximately based on the expression for the coupling system of trinuclear Gd^{3+} in a triangular skeleton,[25] derived from the isotropic Hamiltonian $\mathscr{H} = -2J(\hat{S}_1 \cdot \hat{S}_2 + \hat{S}_1 \cdot \hat{S}_3 + \hat{S}_2 \cdot \hat{S}_3)$. The intertrinuclear interaction was taken into account by using the mean field approximation (zj').[26] The best fit for **4** leads to $J = -0.031\ cm^{-1}$, $g = 1.98$ and $zj' = 0.011\ cm^{-1}$ ($R = 1.83 \times 10^{-5}$). The small and negative J value suggests a very weak antiferromagnetic interaction between Gd^{3+} ions.

The alternating current (ac) susceptibility measurements of **4** performed under a zero direct current (dc) magnetic field and a 3.0 Oe ac field oscillating in the frequency range of 111–3511 Hz reveal that the in-phase signal (χ'_M) hardly shows frequency dependence whereas the out-of-phase signal (χ''_M) can be clearly increased with an increase of the frequency, although no maximum was observed down to 2.0 K (Figure 9a). As the dc field increases at 2 K, the χ'_M signals almost exhibit a continuous decrease up to 20 kOe, but a maximum of χ''_M can be observed at around 3 kOe (Figure 10). With the dc field constants held at 3 kOe, a shoulder around 4 K for χ'_M and a peak at about 3 K for χ''_M are observed in $\chi'_M(T)$ and $\chi''_M(T)$ curves, and are obviously frequency-dependent (Figure 9b). There are antiferromagnetically coupled triangular sublattices within the layered Gd^{3+} wheel-cluster network. Such a frustrated spin geometry has ever been inferred to play a crucial role in the field-induced frequency-dependent magnetic behaviors of some lanthanide complexes.[27] However, with the development in magnetochemistry of lanthanide complexes, this field-induced relaxation process tends to be explained by the magnetic behavior of an isolated ion, the lifting of the Kramer

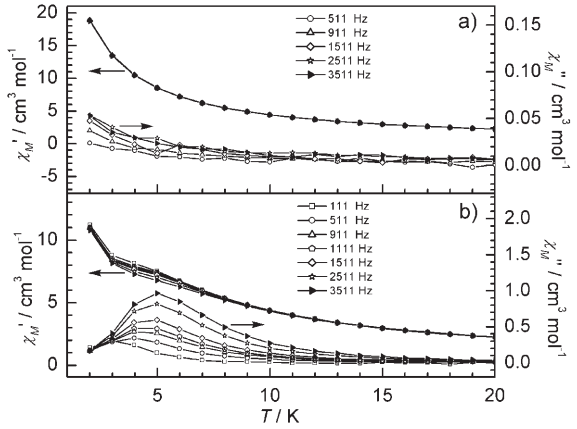

Figure 9. Temperature dependence of the in-phase (χ'_M) and out-of-phase (χ''_M) signals of the ac susceptibility at: a) zero and; b) 3 kOe dc bias field in the frequency range of 111–3511 Hz for **4**.

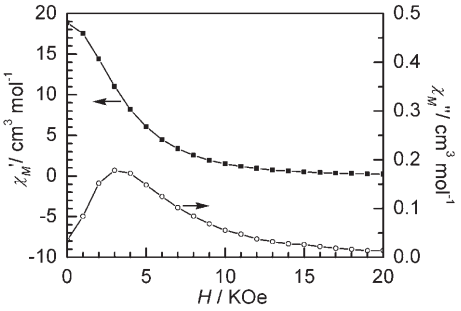

Figure 10. Field-dependent ac magnetic susceptibility of **4** performed at 2 K and 3.0 Oe ac field with a frequency of 911 Hz.

degeneracy by the applied magnetic field is responsible for this magnetic phenomenon.[28] The exchange coupling constant between the adjacent Gd^{3+} ions in **4** is $-0.031\ cm^{-1}$, which is so small that the exchange coupling interaction can be ignored, thus the latter mechanism is more reasonable for explaining this frequency-dependent magnetic behavior in the present system.

Conclusion

We have successfully made a series of novel 3D sandwich frameworks under hydrothermal conditions that contain two distinct layered networks of mixed {Ln_{18}} and {Cu_{24}} wheels. The synthetic procedure has been well established. The unique μ_4-I tetrahedral coordination in the structure plays a key role in forming and stabilizing the {Cu_{24}} wheel and its network; whereas trinuclear [$Ln_3(\mu_3$-O)] cores are responsible for the formation of the {Ln_{18}} wheel and its network. Furthermore, the synergistic coordination between IN and μ_3-O ligands, as well as IN and μ_4-I ligands results in the formation of two distinct networks of {Dy_{18}} and {Cu_{24}} wheel-clusters. The linkages between layered {Ln_{18}} and {Cu_{24}} wheel-cluster networks through IN ligands result in a series of novel Ln-TM sandwich frameworks with multidimension-

al channels. This is the first observation that two different layered networks of nanosized Ln and TM wheels are pillared by IN ligands in wheel-cluster chemistry. It is noticeable that the unusual trinuclear $[Ln_3(\mu_3\text{-}O)]$ and tetranuclear $[Cu_4(\mu_4\text{-}I)]$ cores are successfully used as building blocks to make large oligomers of $\{Ln_{18}\}$ and $\{Cu_{24}\}$ wheels that further link to 2D $\{Ln_{18}\}$ and $\{Cu_{24}\}$ networks, respectively, suggesting that the "oligomerization of low-nuclearity building blocks"[5a] may make larger wheels or wheel-cluster polymers. Further work is in progress to make other new Ln-TM wheels and wheel-cluster polymers by using either larger oligomers of tri- or tetranuclear fragments, or oligomers of higher nuclearity building blocks, whereas simultaneously we are trying to make still larger wheels and wheel-cluster polymers, especially mixed Ln and TM wheels, by selecting another type of ligand or introducing second ligands.

Experimental Section

Materials and physical measurements: All chemicals were purchased from commercial sources and were used without further purification. Elemental analyses for C, H, N were performed on a Vario EL III elemental analyzer. The FTIR spectra (KBr pellets) were recorded by using an ABB Bomen MB 102 spectrometer, and the UV/Vis spectra by using a Lambda900 spectrophotometer. Thermogravimetric analyses were performed on a Mettler TGA/SDTA 851e analyzer with a heating rate of 10 °C min^{-1} under air atmosphere. Photoluminescence analyses were performed by using an Edinburgh Instrument F920 fluorescence spectrometer. The magnetic susceptibilities were measured by using a Quantum Design MPMS-5S superconducting quantum interference device (SQUID) magnetometer in the temperature range of 2–300 K, and the experimental susceptibilities were corrected for the Pascal constants.

Syntheses of 1–7: A mixture of Ln_2O_3 (Y_2O_3 0.113 g, Nd_2O_3 0.168 g, Dy_2O_3 0.189 g; Gd_2O_3 0.181 g; Sm_2O_3 0.174 g; Eu_2O_3 0.176 g; Tb_4O_7 0.187 g), HIN (0.246 g), pca (0.154 g), CuI (0.055 g), H_2O (10 mL), and $HClO_4$ (0.385 mmol, pH 2) was sealed in a 30-mL teflon-lined bomb at 170 °C for seven days which was then slowly cooled to room temperature. Red prismatic crystals of **1–7** and light-yellow rectangular crystals[16] were recovered by filtration, washed with distilled water and dried in air, respectively. Two phases could be manually separated. Interestingly, the syntheses of **1–7** rely on subtle control over various hydrothermal parameters, especially the starting materials (not only pca, but also the I^- ion). It is noteworthy that pca played a critical role in the formation of **1–7**, though pca was not present in **1–7**. When pca was removed from the reaction system, attempts to make **1–7** were unsuccessful under same conditions, except for phase-pure orange crystals which were isomorphous with those in our previous work based on $\{Ln_{14}\}$ cores with iodine bridges.[14a] In addition, a similar reaction that used Cl^- and Br^- ions as halide sources could not produce the isomorphous products of **1–7**, indicating that the I^- ion is indeed critical for the formation of the $\{Cu_{24}\}$ wheel and its network. The larger size of I^- ion induces a coordination number easily up to 4, resulting in a tendency to form tetrahedral coordination. Though the mechanism for forming the $\{Cu_{24}\}$ wheels of **1–7** was unclear, the steric effects involving the size of halide atoms are likely to be responsible for the formation of $\{Cu_{24}\}$ wheel and its network. *Compound* ***1***: Yield (based on Ln_2O_3): 23%; IR (KBr pellet): $\tilde{\nu}$ = 3433(s), 1582(vs), 1541(s), 1439(s), 1402(s), 771 cm^{-1} (m); elemental analysis calcd (%) for $C_{108}H_{75}Cu_8I_5N_{18}O_{39}Y_6$: C 33.05, H 1.93, N 6.42; found: C 32.67, H 2.40, N 6.18. *Compound* ***2***: Yield (based on Ln_2O_3): 29%; IR (KBr pellet): $\tilde{\nu}$3449(s), 1584(vs), 1545(s) 1429(s), 1396(vs), 770 cm^{-1} (m); elemental analysis calcd (%) for $C_{108}H_{75}Cu_8I_5N_{18}Nd_6O_{39}$: C 30.47, H 1.78, N 5.92; found: C 30.02, H 2.22, N 5.73. *Compound* ***3***: Yield (based on Ln_2O_3): 23%; IR (KBr pellet): $\tilde{\nu}$3440(s), 1581(vs), 1546(s), 1436(s) 1401(s), 771 cm^{-1} (m); elemental analysis calcd (%) for $C_{108}H_{75}Cu_8Dy_6I_5N_{18}O_{39}$: C 29.70, H 1.73, N 5.77; found: C 29.51, H 2.17, N 5.67. *Compound* ***4***: Yield (based on Ln_2O_3): 15%; IR (KBr pellet): $\tilde{\nu}$3438(s), 1580(vs), 1546(s), 1434(s) 1397(s), 770 cm^{-1} (m); elemental analysis calcd (%) for $C_{108}H_{75}Cu_8Gd_6I_5N_{18}O_{39}$: C 29.92, H 1.74, N 5.82; found: C 29.85, H 2.13, N 5.78. *Compound* ***5***: Yield (based on Ln_2O_3): 14%; IR (KBr pellet): $\tilde{\nu}$3444(s), 1587(vs), 1543(s), 1433(s) 1397(s), 770 cm^{-1} (m); elemental ayalysis calcd (%) for $C_{108}H_{75}Cu_8Sm_6I_5N_{18}O_{39}$: C 30.21, H 1.76, N 5.87; found: C 29.96, H 2.16, N 5.73. *Compound* ***6***: Yield (based on Ln_2O_3): 12%; IR (KBr pellet): $\tilde{\nu}$3450(s), 1581(vs), 1545(s), 1433(s) 1399(s), 770 cm^{-1} (m); elemental analysis calcd (%) for $C_{108}H_{75}Cu_8Eu_6I_5N_{18}O_{39}$: C 30.14, H 1.76, N 5.86; found: C 29.90, H 2.16, N 5.79. *Compound* ***7***: Yield (based on Ln_2O_3): 10%; IR (KBr pellet): $\tilde{\nu}$3445(s), 1582(vs), 1546(s), 1435(s) 1398(s), 771 cm^{-1} (m); elemental analysis calcd (%) for $C_{108}H_{75}Cu_8Tb_6I_5N_{18}O_{39}$: C 29.85, H 1.74, N 5.80; found: C 29.76, H 2.14, N 5.76.

Crystallographic studies: The intensity data were collected by using a Mercury or SMART-CCD diffractometer with graphite-monochromated $Mo_{K\alpha}$ radiation (λ = 0.71073 Å) at RT. All absorption corrections were performed by using the multiscan or SADABS program. The structures were solved by direct methods and refined by full-matrix least-squares on F^2 with the SHELXTL-97 program package. CCDC-620291, CCDC-620292, CCDC-620297, CCDC-620295, CCDC-620293, CCDC-620294, and CCDC-620296 for **1–7**, respectively, contain the supplementary crystallographic data for this paper. These data can be obtained free of charge from the Cambridge Crystallographic Data Centre via www.ccdc.cam.ac.uk/data_request/cif.

Acknowledgements

This work was supported by the National Natural Science Fund for Distinguished Young Scholar of China (No. 20725101), 973 Program (Nos. 2006CB932900/2006CB932904), the NSF of China (Nos. 20473093), and the NSF of Fujian Province (No. E0510030).

[1] a) A. Tsuda, E. Hirahara, Y.-S. Kim, H. Tanaka, T. Kawai, T. Aida, *Angew. Chem.* **2004**, *116*, 6487; *Angew. Chem. Int. Ed.* **2004**, *43*, 6327; b) D.-L. Long, L. Cronin, *Chem. Eur. J.* **2006**, *12*, 3698.

[2] a) E. Cadot, F. Sécheresse, *Chem. Commun.* **2002**, 2189; b) J. Overgaard, B. B. Iversen, S. P. Palii, G. A. Timco, N. V. Gerbeleu, F. K. Larsen, *Chem. Eur. J.* **2002**, *8*, 2775; c) D.-L. Long, H. Abbas, P. Kögerler, L. Cronin, *J. Am. Chem. Soc.* **2004**, *126*, 13880; d) S. S. Mal, U. Kortz, *Angew. Chem.* **2005**, *117*, 3843; *Angew. Chem. Int. Ed.* **2005**, *44*, 3777.

[3] A. Müller, C. Serain, *Acc. Chem. Res.* **2000**, *33*, 2.

[4] a) A. J. Tasiopoulos, A. Vinslava, W. Wernsdorfer, K. A. Abboud, G. Christou, *Angew. Chem.* **2004**, *116*, 2169; *Angew. Chem. Int. Ed.* **2004**, *43*, 2117; b) M. Murugesu, J. Raftery, W. Wernsdorfer, G. Christou, E. K. Brechin. *Inorg. Chem.* **2004**, *43*, 4203; c) D. Foguet-Albiol, T. A. O'Brien, W. Wernsdorfer, B. Moulton, M. J. Zaworotko, K. A. Abboud, G. Christou, *Angew. Chem.* **2005**, *117*, 919; *Angew. Chem. Int. Ed.* **2005**, *44*, 897.

[5] a) A. L. Dearden, S. Parsons, R. E. P. Winpenny, *Angew. Chem.* **2001**, *113*, 155; *Angew. Chem. Int. Ed.* **2001**, *40*, 152; b) C. Cadiou, M. Murrie, C. Paulsen, V. Villar, W. Wernsdorfer, R. E. P. Winpenny, *Chem. Commun.* **2001**, 2666.

[6] a) C.- H. Chang, K.-C. Hwang, C.-S. Liu, Y. Chi, A. J. Carty, L. Scoles, S.-M. Peng, G.-H. Lee, J. Reedijk, *Angew. Chem.* **2001**, *113*, 4787; *Angew. Chem. Int. Ed.* **2001**, *40*, 4651; b) G. Mezei, P. Baran, R. G. Raptis, *Angew. Chem.* **2004**, *116*, 584; *Angew. Chem. Int. Ed.* **2004**, *43*, 574; c) X.-C. Huang, J.-P. Zhang, X.-M. Chen, *J. Am. Chem. Soc.* **2004**, *126*, 13218.

[7] a) K. L. Taft, C. D. Delfs, G. C. Papaefthymiou, S. Foner, D. Gatteschi, S. J. Lippard, *J. Am. Chem. Soc.* **1994**, *116*, 823; b) S. P. Watton, P. Fuhrmann, L. E. Pence, A. Caneschi, A. Cornia, G. L. Abbati,

S. J. Lippard, *Angew. Chem.* **1997**, *109*, 2917; *Angew. Chem. Int. Ed. Engl.* **1997**, *36*, 2774; c) C. P. Raptopoulou, V. Tangoulis, E. Devlin, *Angew. Chem.* **2002**, *114*, 2492; *Angew. Chem. Int. Ed.* **2002**, *41*, 2386; d) O. L. Sydora, P. T. Wolczanski, E. B. Lobkovsky, *Angew. Chem.* **2003**, *115*, 2789; *Angew. Chem. Int. Ed.* **2003**, *42*, 2685; e) O. L. Sydora, T. P. Henry, P. T. Wolczanski, E. B. Lobkovsky, E. Rumberger, D. N. Hendrickson, *Inorg. Chem.* **2006**, *45*, 609, and references therein.

[8] E. K. Brechin, O. Cador, A. Caneschi, C. Cadiou, S. G. Harris, S. Parsons, M. Vonci, R. E. P. Winpenny, *Chem. Commun.* **2002**, 1860.

[9] D. M. Low, G. Rajaraman, M. Helliwell, G. Timco, J. v. Slageren, R. Sessoli, S. T. Ochsenbein, R. Bircher, C. Dobe, O. Waldmann, H. U. Güdel, M. A. Adams, E. Ruiz, S. Alvarez, E. J. L. McInnes, *Chem. Eur. J.* **2006**, *12*, 1385, and references therein.

[10] R. H. Laye, M. Murrie, S. Ochsenbein, A. R. Bell, S. J. Teat, J. Raftery, H. U. Güdel, E. J. L. McInnes, *Chem. Eur. J.* **2003**, *9*, 6215.

[11] a) O. Poncelet, L. G. Hubert-Pfalzgraf, J.- C. Daran, R. Astier, *J. Chem. Soc. Chem. Commun.* **1989**, 1846; b) R. Anwander, *Angew. Chem.* **1998**, *110*, 619; *Angew. Chem. Int. Ed.* **1998**, *37*, 599; c) R. Wang, Z. Zheng, T. Jin, R. J. Staples, *Angew. Chem.* **1999**, *111*, 1929; *Angew. Chem. Int. Ed.* **1999**, *38*, 1813; d) Z. Zheng. *Chem. Commun.* **2001**, 2521; e) Y. Bretonnière, M. Mazzanti, J. Pécaut, M. M. Olmstead, *J. Am. Chem. Soc.* **2002**, *124*, 9012; f) L. G. Westin, M. Kritikos A. Caneschi, *Chem. Commun.* **2003**, 1012; g) T. Kajiwara, H. Wu, T. Ito, N. Iki, S. Miyano, *Angew. Chem.* **2004**, *116*, 1868; *Angew. Chem. Int. Ed.* **2004**, *43*, 1832; h) T. Kajiwara, K. Katagiri, S. Takaishi, M. Yamashita, N. Iki, *Chem. Asian J.* **2006**, *1*, 349.

[12] Z. Ni, H. Kou, L. Zhang, C. Ge, A. Cui, R. Wang, Y. Li, O. Sato, *Angew. Chem.* **2005**, *117*, 7920; *Angew. Chem. Int. Ed.* **2005**, *44*, 7742.

[13] a) F. K. Larsen, E. J. L. McInnes, H. E. Mkami, J. Overgaard, S. Piligkos, G. Rajaraman, E. Rentschler, A. A. Smith, V. Boote, M. Jennings, G. A. Timko, R. E. P. Winpenny, *Angew. Chem.* **2003**, *115*, 105; *Angew. Chem. Int. Ed.* **2003**, *42*, 101; b) E. J. L. McInnes, S. Piligkos, G. A. Timco, R. E. P. Winpenny, *Coord. Chem. Rev.* **2005**, *249*, 2577, and references therein; c) S. L. Heath, R. H. Laye, C. A. Muryn, N. Lima, R. Sessoli, R. Shaw, S. J. Teat, G. A. Timco, R. E. P. Winpenny, *Angew. Chem.* **2004**, *116*, 6258; *Angew. Chem. Int. Ed.* **2004**, *43*, 6132; d) O. Cador, D. Gatteschi, R. Sessoli, F. K. Larsen, J. Overgaard, A.-L. Barra, S. J. Teat, G. A. Timco, R. E. P. Winpenny, *Angew. Chem.* **2004**, *116*, 5308; *Angew. Chem. Int. Ed.* **2004**, *43*, 5196; e) F. K. Larsen, J. Overgaard, S. Parsons, E. Rentschler, A. A. Smith, G. A. Timco, R. E. P. Winpenny, *Angew. Chem.* **2003**, *115*, 6160; *Angew. Chem. Int. Ed.* **2003**, *42*, 5978; f) R. H. Laye, F. K. Larsen, J. Overgaard, C. A. Muryn, E. J. L. McInnes, E. Rentschler, V. Sanchez, S. J. Teat, H. U. Güdel, O. Waldmann, G. A. Timco, R. E. P. Winpenny, *Chem. Commun.* **2005**, 1125; g) G. Timco, A. S. Batsanov, F. K. Larsen, C. A. Muryn, J. Overgaard, S. J. Teat, R. E. P. Winpenny, *Chem. Commun.* **2005**, 3648; h) M. Affronte, I. Casson, M. Evangelisti, A. Candini, S. Carretta, C. A. Muryn, S. J. Teat, G. A. Timco, W. Wernsdorfer, R. E. P. Winpenny, *Angew. Chem.* **2005**, *117*, 6654; *Angew. Chem. Int. Ed.* **2005**, *44*, 6496; i) M. Affronte, F. Troiani, A. Ghirri, S. Carretta, P. Santini, V. Corradini, R. Schuecker, C. A. Muryn, G. Timco, R. E. P. Winpenny, *Dalton Trans.* **2006**, 2810; j) M. Affronte, S. Carretta, G. A. Timco, R. E. P. Winpenny, *Chem. Commun.* **2007**, 1789.

[14] a) M.-B. Zhang, J. Zhang, S.-T. Zheng, G.-Y. Yang, *Angew. Chem.* **2005**, *117*, 1409; *Angew. Chem. Int. Ed.* **2005**, *44*, 1385; b) J.-W. Cheng, J. Zhang, S.-T. Zheng, M.-B. Zhang, G.-Y. Yang, *Angew. Chem.* **2006**, *118*, 79; *Angew. Chem. Int. Ed.* **2006**, *45*, 73.

[15] a) A. Müller, S. K. Das, H. Bögge, C. Beugholt, M. Schmidtmann, *Chem. Commun.* **1999**, 1035; b) A. Müller, E. Krichemeyer, H. Bögge, M. Schmidtmann, C. Beugholt, S. K. Das, F. Peters, *Chem. Eur. J.* **1999**, *5*, 1496, and references therein.

[16] Light yellow rectangular crystals: $[Dy_2(pca)(IN)_6Cu_5I_4(H_2O)_2]\cdot H_2O$ (Dy-Cu), orthorhombic, $Pca2_1$, $a=21.296(2)$, $b=7.2116(7)$, $c=35.191(4)$ Å, $V=5404.5(9)$ Å^3, $Z=4$. X-ray crystal structure analyses show that the existence of Dy–pca layers and Cu–I chains which are further pillared by IN ligands. Other Ln–Cu analogous to Dy–Cu were also obtained (CCDC-621167–CCDC-621172 for Y, Gd, Tb, Dy, Er, Yb, respectively). Full details of the structures, discussion of the reaction with different starting materials, and the fluorescent and magnetic properties of these compounds will be published later.

[17] T. Loiseau, L. Lecroq, C. Volkringer, J. Marrot, G. Férey, M. Haouas, F. Taulelle, S. Bourrelly, P. L. Llewelly, M. Latroche, *J. Am. Chem. Soc.* **2006**, *128*, 10223, and references therein.

[18] J. Gromada, A. Mortreux, T. Chenal, J. W. Ziller, F. Leising, J.-F. Carpentier, *Chem. Eur. J.* **2003**, *9*, 3773, and references therein.

[19] a) T. S. Lobana, P. Kaur, T. Nishioka, *Inorg. Chem.* **2004**, *43*, 3766; b) T. Wu, D. Li, S. W. Ng, *CrystEngComm* 2005, 7, 514.

[20] a) G.-Y. Yang, S. C. Sevov, *J. Am. Chem. Soc.* **1999**, *121*, 8389; b) J. Yu, R. Xu, *Chem. Soc. Rev.* **2006**, *35*, 593.

[21] P. Feng, X. Bu, N. Zheng, *Acc. Chem. Res.* **2005**, *38*, 293.

[22] J. Yang, Q. Yue, G.-D. Li, J.-J. Cao, G.-H. Li, J.-S. Chen, *Inorg. Chem.* **2006**, *45*, 2857.

[23] J.-K. Cheng, Y.-G. Yao, J. Zhang, Z.-J. Li, Z.-W. Cai, X.-Y. Zhang, Z.-N. Chen, Y. B. Chen, Y. Kang, Y.-Y. Qin, Y.-H. Wen, *J. Am. Chem. Soc.* **2004**, *126*, 7796.

[24] a) J.-P. Costes, F. Nicode, *Chem. Eur. J.* **2002**, *8*, 3442; b) M. Andruh, E. Bakalbassis, O. Kahn, J. C. Trombe, P. Porchers, *Inorg. Chem.* **1993**, *32*, 1616.

[25] a) Y.-T. Li, P. Cheng, D.-Z. Liao, Z.-H. Jiang, S.-P. Yan, G.-L. Wang, *Synth. React. Inorg. Met.-Org. Chem.* **1996**, *26*, 409; b) K. Kambe, *J. Phys. Soc. Jpn.* **1950**, *5*, 48.

[26] B. E. Myers, L. Berger, S. A. Friedberg, *J. Appl. Phys.* **1969**, *40*, 1149.

[27] B. Ma, S. Gao, G. Su, G. Xu, *Angew. Chem.* **2001**, *113*, 448; *Angew. Chem. Int. Ed.* **2001**, *40*, 434.

[28] a) M. Sugita, N. Ishikawa, T. Ishikawa, S. Koshihara, Y. Kaizu, *Inorg. Chem.* **2006**, *45*, 1299; b) Y.-Z. Zhang, G.-P. Duan, O. Sato, S. Gao, *J. Mater. Chem.* **2006**, *16*, 2625.

Received: April 19, 2007
Published online: October 2, 2007

